STUDY OF COLLECTIVE EFFECTS IN THE CERN FCC-EE TOP-UP BOOSTER

D. Quartullo*, INFN-Rome1, Rome, Italy
M. Migliorati, Sapienza University and INFN-Rome1, Rome, Italy
M. Zobov, LNF-INFN, Frascati, Italy

Abstract

The CERN FCC-ee top-up booster synchrotron will accelerate electrons and positrons from an injection energy of 20 GeV up to an extraction energy between 45.6 GeV and 182.5 GeV depending on the operation mode. These accelerated beams will be used for the initial filling of the high-luminosity FCC-ee collider and for keeping constant the beam current over time using continuous top-up injection. Due to the high-intensities of the circulating beams, collective effects may represent a limitation in the top-up booster. In this work we present a first evaluation of the impedance model and the effects on beam dynamics. Methods to mitigate possible instabilities will be also discussed.

INTRODUCTION

The CERN e^+e^- Future Circular Collider (FCC-ee) is a high-luminosity and high-precision electron-positron circular collider envisioned in a 100 km tunnel in the CERN-Geneva area [1]. The FCC-ee will allow detailed studies of the heaviest known particles (Z, W, H bosons and the top quark) offering also great sensitivity to new particle physics.

The FCC-ee target luminosities of $10^{34} - 10^{36}$ cm^{-2} s^{-1} will lead to short beam lifetimes, due to beamstrahlung, radiative Bhabha scattering and Touschek effect [1]. In order to sustain these short beam lifetimes, a full-energy booster will provide continuous top-up injection, in addition to initially filling the FCC-ee.

The booster will be built in the same tunnel used for the collider and the circumference lengths of the two machines will be the same, almost 100 km. The booster will accelerate batches of electrons and positrons from an injection energy of 20 GeV up to an extraction energy of 45.6 GeV, 80 GeV, 120 GeV, 182.5 GeV for Z, W, H and top quark production, respectively [1]. This design injection energy, which corresponds to a magnetic field $B = 6$ mT, could change in the future, depending on the quality and reproducibility of the magnetic field in the dipole magnets.

In order not to affect the collider luminosity and to diminish the background generated by lost particles, the booster is expected to provide, at extraction, an equilibrium transverse emittance similar to the one in the collider. Since the FCC-ee lattice will be optimized for two optics, one with 60° phase advance for the Z and W experiments, the other with 90° phase advance for the H and top quark productions, the optics in the booster will change depending on the phase advance in the collider.

* Danilo.Quartullo@roma1.infn.it

The synchrotron radiation (SR) transverse damping time at booster injection-energy will be longer than 10 s, leading to incompatibility with the booster cycle [2]. In addition, the horizontal normalized equilibrium emittance of 12 pm rad will cause emittance blow-up along the cycle due to intra-beam scattering. In order to solve these issues, 16 wigglers should be installed in the booster, leading to a damping time of 0.1 s and an emittance of 240 pm rad and 180 pm rad for the 60° and 90° optics respectively.

The high nominal intensity of $N_b = 3.4{\times}10^{10}$ particles per bunch (ppb) could lead to collective effects able to severely limit the booster operation. In particular, the resistive wall effect, due to the foreseen beam-pipe in stainless steel with radius $r_c = 25$ mm, could cause strong instabilities in both longitudinal and transverse planes.

The importance of collective effects in the booster at injection energy was already reported in Ref. [3], where it was shown that, without wigglers, an intensity threshold of 0.1×10^{10} ppb, significantly lower than the nominal intensity, was defined by the microwave instability (MI) caused by the resistive wall impedance. In the transverse plane, the intensity threshold due to transverse mode-coupling instability (TMCI) was only 0.6×10^{10} ppb. Moreover, analytical estimations of the resistive wall transverse coupled-bunch instability (TCBI) found a rise time of just few revolution turns which requires new feedback schemes [4].

This work aims at finding possible cures to the impedance-induced instabilities in the booster, focusing on the beam dynamics at injection energy and assuming an optics with 60° phase advance and no wigglers installed in the machine.

The next section highlights the machine and beam parameters considered in the present study. Then, careful estimations of the resistive-wall impedance are given, together with a possible way to lower it. The work continues studying the MI in the longitudinal plane through macroparticle simulations, providing a possible cure to increase the intensity threshold. Subsequently, choosing a proper combination of parameters which allows having stable beams at the nominal intensity, the study shifts to the transverse plane, where a semi-analytical Vlasov solver is used to find the TMCI intensity threshold. Finally, estimations of the TCBI rise-time are provided using analytical formulae.

MACHINE AND BEAM PARAMETERS CONSIDERED IN THE STUDY

Table 1 shows the machine and beam parameters used in the study of collective effects in the booster.

Table 1: Main machine and beam parameters relevant for the booster studies. Most of these quantities can be found in Ref. [1].

Parameter	Value
Machine circumference (C_r)	97.756 km
Beam energy at injection (E_0)	20 GeV
Beam rev. frequency at injection (f_0)	3.06 kHz
Nominal bunch intensity (N_b^{nom})	3.4×10^{10} ppb
Number of bunches per beam (M_b)	16640
SR 1 σ rel. energy spread ($\sigma_{dE0,r}$)	0.166×10^{-3}
SR energy loss per turn (U_0)	1.33 MeV
SR longitudinal damping time (τ_z)	15013 turns
SR 1 σ long. bunch length (σ_{z0})	1.26 mm
RF frequency (f_{rf})	400 MHz
Harmonic number (h)	130432
RF voltage (V_{rf})	60 MV
Arc phase advance (ϕ_a)	60°
Momentum compaction factor (α_c)	1.48×10^{-5}
Synchrotron tune (Q_s)	0.0304
Betatron tunes ($Q_{x,y}^{nom}$)	269.139

As shown below, the study of the booster beam dynamics at injection energy is the most critical as concerns intensity effects in both the longitudinal and transverse planes.

The considered $\phi_a = 60°$ directly determines α_c and influences Q_s and σ_{z0}. As reported later, the MI intensity threshold is proportional to α_c and σ_{z0} while the TMCI intensity threshold is proportional to Q_s. A phase advance of 90° would lead to lower values for α_c, Q_s, σ_{z0} and therefore to more critical scenarios.

The main three SR parameters σ_{z0}, U_0 and τ_z can be directly computed assuming an average dipole-magnet bending radius $\rho_b = 10.6$ km in the absence of wigglers.

The booster main RF system consists of 400 MHz superconducting cavities [1]. In the present work, a voltage $V_{rf} = 60$ MV at injection energy is assumed. This value is significantly higher than U_0 so that the bunch sees the linear part of the RF voltage at each revolution turn. In addition, the chosen V_{rf} is expected to be substantially lower than the total available voltage, so that V_{rf} can be increased during acceleration according to the cycle needs.

The number of bunches simultaneously accelerated in the booster will depend on the collider experiment. Table 1 indicates the largest planned M_b, which relates to the Z-boson experiment [1].

Concerning the transverse plane, the horizontal and vertical tunes are assumed to be equal to the horizontal tune foreseen in the FCC-ee for the Z-boson experiment [1].

ESTIMATION OF THE RESISTIVE WALL IMPEDANCE

The resistive wall impedance is the dominant component of the booster impedance model and it is the only impedance contribution considered in this paper.

The baseline for costs minimization is to have a circular beam-pipe in stainless steel (resistivity $\rho_r = 7 \times 10^{-7} \Omega$m) with radius $r_c = 25$ mm. However, the corresponding resistive wall impedance would lead to a peak induced voltage even higher than the peak RF voltage for a bunch with the nominal intensity, see Fig. 1.

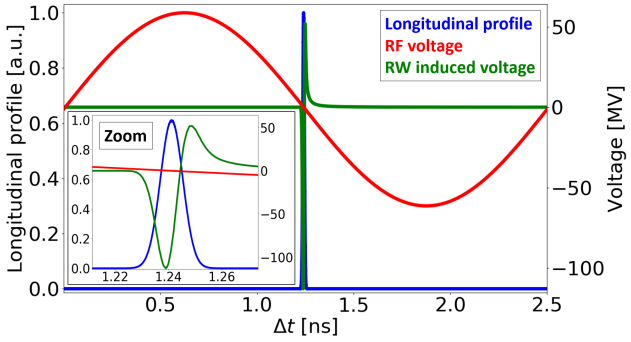

Figure 1: Longitudinal profile (blue), RF voltage (red) and resistive wall induced voltage (green) as a function of time in the FCC-ee booster considering the parameters in Table 1 and a stainless steel beam pipe with radius $r_c = 25$ mm.

In order to reduce this impedance, the possibility of applying a copper coating to the beam-pipe was investigated. Specifically, the CERN IW2D code [5] was used to evaluate the longitudinal and transverse resistive wall impedances of a two-layer vacuum chamber, being the external layer in stainless steel and the internal layer in copper ($\rho_r = 1.7 \times 10^{-8} \Omega$m) with variable thickness δ_l, see Fig. 2.

For single-layer beam-pipes, the dependences of the longitudinal and transverse-dipolar resistive wall impedances on the frequency are [6]

$$|Z_\parallel(f)| \propto \frac{1}{r_c}\sqrt{\rho_r f}, \quad |Z_{x,y}(f)| \propto \frac{1}{r_c^3}\sqrt{\frac{\rho_r}{f}} \qquad (1)$$

in a certain asymptotic range of frequencies. These dependencies are highlighted in Fig. 2, where all the axes are in logarithmic scale.

The plots in Fig. 2 also show that, for a given δ_l, both longitudinal and transverse impedances converge to the single-layer stainless-steel and copper impedances respectively for low and high frequencies. In particular, for a given δ_l, the two frequencies where the longitudinal and transverse impedances converge to the corresponding single-layer copper impedances are essentially the same and will be denoted by f_{δ_l} below.

In the next section, the MI thresholds will be evaluated for the different impedances shown in Fig. 2 (top). As reported in Ref. [7], MI can occur when the wavelength of the wake-field is much shorter than the bunch length, i.e. $f_c\tau \gg 1$, where f_c is the frequency of the impedance which drives MI and τ is the full bunch length. Therefore, it is expected that the impedance related to a given δ_l and the impedance of the single-layer copper beam-pipe will lead to the same MI intensity threshold if these two impedances coincide for frequencies larger than $1/\tau$, i.e. when $f_{\delta_l} < 1/\tau$.

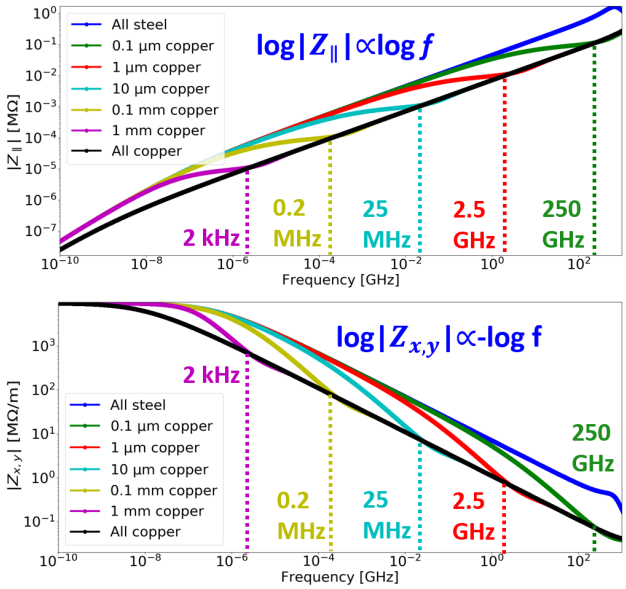

Figure 2: Longitudinal (top) and transverse dipolar (bottom) resistive wall impedance as a function of frequency in the FCC-ee booster assuming a beam-pipe in stainless steel with radius $r_c = 25$ mm and different values for the thickness of the internal copper layer. The five vertical dashed lines mark the frequencies f_{δ_l} above which the corresponding impedances converge to the single-layer copper impedance. The dependences of the single-layer impedances on the frequency are also reported in both plots. All the impedance curves have been obtained with the IW2D code.

Finally, it should be noted that, being the booster a fast-cycling machine, eddy currents in presence of a copper layer could be an issue during acceleration and their effects should be separately investigated.

CURES FOR INCREASING THE MICROWAVE-INSTABILITY INTENSITY THRESHOLD

Single-bunch macroparticle longitudinal beam dynamics simulations were performed with the CERN BLonD code [8] in order to evaluate the MI intensity threshold ($N^{\mathrm{MI}}_{b,\mathrm{th}}$) taking into account the parameters of Table 1 and the resistive-wall impedance shown in Fig. 2 (top) with a variable δ_l.

Simulation tracking lasted 10^6 revolution turns, which is more than 6 times the SR longitudinal damping time, in such a way to reach a SR equilibrium at the end of simulations. It should be noted that 10^6 turns corresponds to 32.6 s, which is comparable to the flat-bottom duration of 51.1 s in the booster for the Z-boson experiment [1].

The resistive-wall induced voltage was computed in frequency domain, multiplying the bunch spectrum by the impedance and performing an inverse Fourier transform. Due to the short bunches and to have an acceptable resolution in the longitudinal profile binning (at least 50 slices for 4-σ bunch length), the maximum frequency considered in computations was 500 GHz. This obliged to use a large number of macroparticles per bunch (more than 10^7) in order to counteract the numerical noise obtained when multiplying impedance and bunch spectrum, which are increasing and decreasing functions of frequency, respectively (Fig. 3).

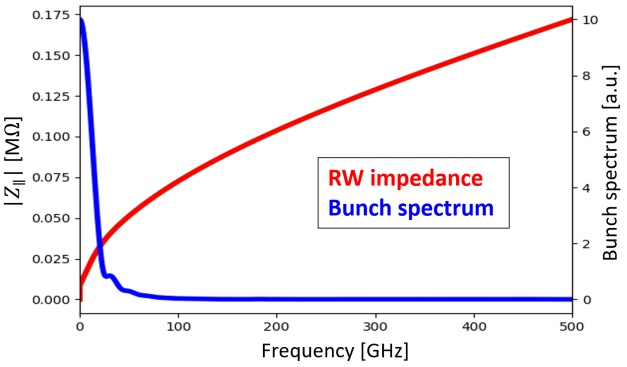

Figure 3: Resistive wall impedance and bunch spectrum used to compute the induced voltage in BLonD simulations. Case of $\delta_l = 1\mu$m, $\sigma_z = 4$ mm at SR equilibrium.

Figure 4 shows the simulation results, specifically the equilibrium $\sigma_{dE,\mathrm{r}}$ and σ_z (averaged over the last 10000 revolution turns) as a function of N_b and varying δ_l.

When observed in simulation, MI led to a $\sigma_{dE,\mathrm{r}}$ increase relative to $\sigma_{dE0,\mathrm{r}}$. More specifically, up to a certain intensity threshold $N^{\mathrm{MI}}_{\mathrm{b,th}}$, $\sigma_{dE,\mathrm{r}} \approx \sigma_{dE0,\mathrm{r}}$, while $\sigma_{dE,\mathrm{r}}$ becomes an increasing function of N_b when $N_\mathrm{b} > N^{\mathrm{MI}}_{\mathrm{b,th}}$. In Fig. 4 (top), to unambiguously determine $N^{\mathrm{MI}}_{\mathrm{b,th}}$, the MI intensity threshold is chosen so that, when $N_\mathrm{b} = N^{\mathrm{MI}}_{\mathrm{b,th}}$, then $\sigma_{dE,\mathrm{r}} = 1.1\sigma_{dE0,\mathrm{r}}$.

Figure 4 (top) shows that, even with a beam-pipe entirely made of copper, the threshold $N^{\mathrm{MI}}_{\mathrm{b,th}}$ is only 1.5×10^{10} ppb, significantly lower than the nominal bunch intensity. This value for $N^{\mathrm{MI}}_{\mathrm{b,th}}$ can be also obtained with good approximation when $\delta_l = 1\mu$m.

Concerning the equilibrium bunch length, Fig. 4 (bottom) shows that σ_z is an increasing function of N_b and the bunch lengthening relative to σ_{z0} is higher when the resistive-wall impedance is larger (smaller δ_l). This bunch lengthening occurs even when $N_\mathrm{b} < N^{\mathrm{MI}}_{\mathrm{b,th}}$ and no clear changes in curve behaviour are visible in correspondence of $N_\mathrm{b} = N^{\mathrm{MI}}_{\mathrm{b,th}}$.

With a vacuum-chamber entirely in copper, the equilibrium full bunch-length is $\tau \approx 4\sigma_z = 36$ ps when $N_\mathrm{b} = 1.5 \times 10^{10}$ ppb (Fig. 4, bottom). Therefore, following the reasoning of the previous section, a copper coating should lead to the highest possible MI intensity-threshold (1.5×10^{10} ppb) when $f_{\delta_l} < 1/\tau \approx 30$ GHz. This is in good agreement with the f_{δ_l} values reported in Fig. 2 (top), since f_{δ_l} is larger than 30 GHz when $\delta_l = 0.1\mu$m and lower than 30 GHz when $\delta_l = 1\mu$m.

Since the reduction of the longitudinal resistive-wall impedance by adding a copper layer to the beam-pipe did not avoid MI for the nominal bunch intensity, a second cure for instability has been studied.

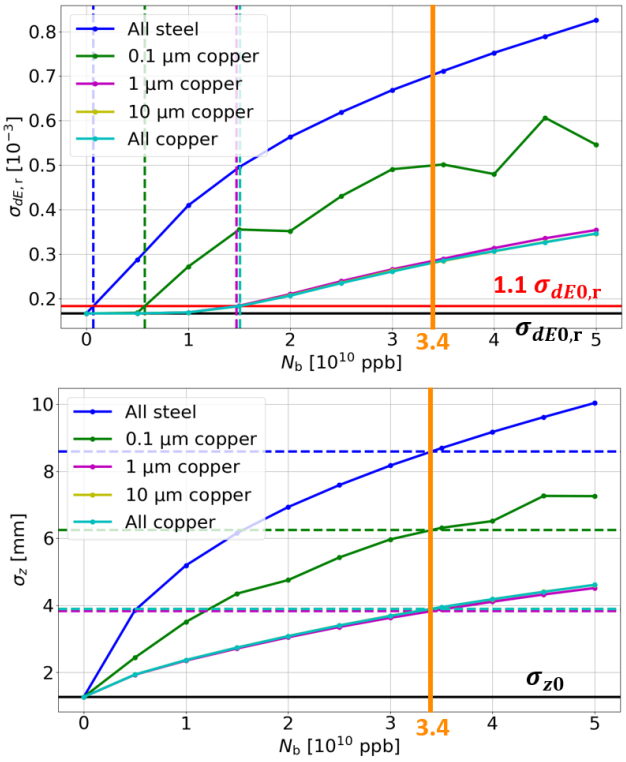

Figure 4: Equilibrium rms relative energy spread (top) and bunch length (bottom) as a function of bunch intensity obtained with BLonD simulations. The used parameters are reported in Table 1 and the resistive wall impedance shown in Fig. 2 (top) has been included in simulations varying δ_l. Top: the horizontal lines mark $\sigma_{dE0,r}$ and its increase by 10%. The dashed vertical lines mark $N_{b,th}^{MI}$ for the corresponding curves. Bottom: the black line marks σ_{z0}, while the dashed horizontal lines indicate the values of σ_z when $N_b = 3.4\times10^{10}$ ppb and δ_l varies. In both images the yellow and cyan curves are overlapped.

For the Boussard criterion [9], $N_{b,th}^{MI}$ scales as

$$N_{b,th}^{MI} \propto \frac{\alpha_c E_0 \sigma_{dE0,r}^2 \sigma_{z0}}{|Z_\parallel|/n}, \qquad (2)$$

where $n = f/f_0$. As expected, this expression shows that the MI intensity threshold increases when the longitudinal resistive wall impedance is reduced. Equation (2) clarifies also the observation done above concerning the major strength of MI at booster injection-energy with the 90° phase-advance optics (lower α_c). Moreover, Eq. (2) shows that $N_{b,th}^{MI}$ depends quadratically on $\sigma_{dE0,r}$ and linearly on σ_{z0}.

One way to increase $\sigma_{dE0,r}$ consists in installing wigglers in the booster with a consequent increase in U_0. Indeed, the two scaling relations [10]

$$\tau_z = \frac{1}{U_0(1+C_1U_0)}, \quad \sigma_{dE0,r} \propto \sqrt{\frac{U_0}{1+C_2U_0}}, \qquad (3)$$

where C_1 and C_2 are positive quantities not depending on U_0, show that a larger U_0 leads to lower τ_z and higher $\sigma_{dE0,r}$.

Therefore, the BLonD simulations were repeated varying U_0 and considering $\delta_l = 1\,\mu$m, which is a compromise between an increase in $N_{b,th}^{MI}$ (Fig. 4, top) and a decrease in production costs and potential eddy-current issues related to the copper-layer thickness.

Figure 5 (top) shows the new intensity thresholds. As foreseen by Eqs. (2) and (3), the plot shows that $N_{b,th}^{MI}$ increases with U_0. In particular, values of U_0 not larger than 3 MeV lead to MI for the nominal bunch intensity.

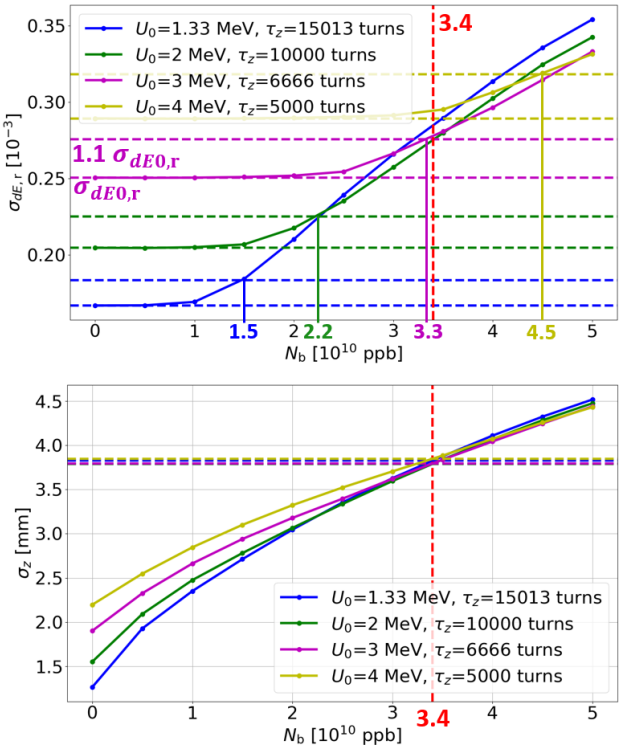

Figure 5: Equilibrium rms relative energy spread (top) and bunch length (bottom) as a function of bunch intensity obtained with BLonD simulations. The used parameters are reported in Table 1, except for the SR quantities which vary following Eq. (3). The resistive wall impedance with $\delta_l = 1\,\mu$m (Fig. 2, top) has been included in simulations. Top: for each curve, the corresponding horizontal lines mark $\sigma_{dE0,r}$ and its increase by 10%, while the vertical line marks $N_{b,th}^{MI}$. Bottom: the horizontal lines indicate the values of σ_z when $N_b = 3.4\times10^{10}$ ppb and U_0 varies.

Regarding the bunch lengths, Fig. 5 (bottom) shows that σ_{z0} increases as a function of U_0, helping in increasing $N_{b,th}^{MI}$ as Eq. (2) suggests. The plot also indicates that the increase of σ_z with U_0 is less and less significant as N_b approaches the nominal bunch intensity.

This second additional cure for MI, i.e. installing wigglers in the booster to increase U_0, is in full agreement with the current machine design-plan. Indeed, as already mentioned above, considerations concerning the transverse plane would lead to the installation of 16 wigglers able to provide $U_0 =$ 126 MeV [1,2]. Simulations with such a value for U_0 require a much larger V_{rf}, moreover there would be likely no need to

add a copper layer to the beam pipe due to the larger $\sigma_{dE0,\mathrm{r}}$ in Eq. (2). Further studies are needed to cover this scenario.

TRANSVERSE MODE-COUPLING INSTABILITY INTENSITY THRESHOLD

The previous section showed that a bunch with nominal intensity does not suffer MI when $U_0 = 4$ MeV and $\delta_\mathrm{l} = 1\,\mu$m. Taking into account these two conditions, beam dynamics studies in the transverse plane were needed to verify that the bunch is not unstable due to TMCI.

The intensity threshold for TMCI scales as [11]

$$N_{\mathrm{b,th}}^{\mathrm{TMCI}} \propto \frac{Q_{x,y} Q_s E_0 \sigma_z}{\mathrm{Im}(Z_{x,y})}, \qquad (4)$$

where $\mathrm{Im}(Z_{x,y})$ is the imaginary part of the transverse resistive-wall impedance.

The quantity $\mathrm{Im}(Z_{x,y})$ was decreased adding a copper-layer to the beam pipe in order to cope with MI. Equation (4) shows a linear dependence of $N_{\mathrm{b,th}}^{\mathrm{TMCI}}$ on the equilibrium σ_z which, for a certain U_0, increases with N_b (see bottom plots in Figs. 4 and 5). This bunch-lengthening in the longitudinal plane helps increasing $N_{\mathrm{b,th}}^{\mathrm{TMCI}}$. Note also that, at least for bunch intensities close to or above the nominal value, increasing U_0 would not lengthen the bunch (Fig. 5, bottom) and therefore would not help to counteract TMCI.

The CERN DELPHI code [12], which is a semi-analytical Vlasov solver for impedance-driven modes, was used to evaluate $N_{\mathrm{b,th}}^{\mathrm{TMCI}}$ without taking into account the radiation damping. The values for σ_z needed in DELPHI have been taken from the BLonD simulation results described above (yellow curve in the bottom plot of Fig. 5).

Figure 6 shows the real and imaginary parts of the complex tune shift of the first coherent oscillation modes obtained with DELPHI.

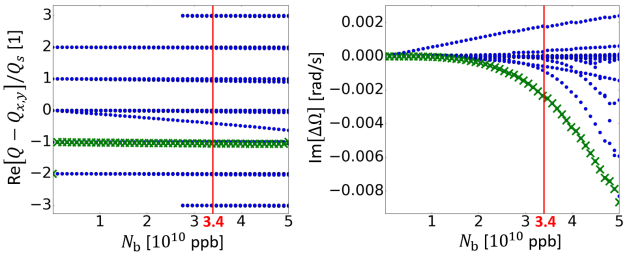

Figure 6: Real (left) and imaginary (right) parts of the tune shift of the first coherent oscillation modes as a function of the bunch intensity obtained with DELPHI. In both plots the green cross associated to a given N_b marks the unstable mode with largest growth rate. The parameters needed in simulation are taken from Table 1, except for the equilibrium σ_z which depends on N_b according to the yellow curve in Fig. 5 (bottom, $U_0 = 4$ MeV). The value $\delta_\mathrm{l} = 1\,\mu$m is assumed for the dipolar resistive-wall impedance.

No mode coupling occurs up to $N_\mathrm{b} = 5\times10^{10}$ ppb (Fig. 6, left). In addition, the rise times of the unstable modes (Fig. 6, right) are longer than 125 s, and these values are large compared to the SR transverse damping-time (3.26 s) and the flat-bottom durations in the booster, which vary from 1.6 s to 51.1 s according to the collider experiment [1].

Therefore, $N_{\mathrm{b,th}}^{\mathrm{TMCI}} > 5\times10^{10}$ ppb and, in particular, no TMCI is observed for the nominal bunch intensity. Figure 7 shows 20 consecutive transverse-amplitude (Head-Tail) signals obtained with DELPHI when $N_\mathrm{b} = N_\mathrm{b}^{\mathrm{nom}}$. Notice that the mode -1 largely prevails while the mode 0 only creates an asymmetry between the amplitudes of the two signal halves.

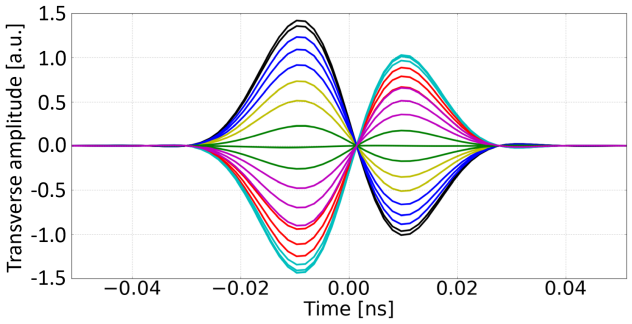

Figure 7: Twenty consecutive Head-Tail signals as a function of the longitudinal coordinate (0 ns corresponds to the bunch centre). These signals were obtained with DELPHI and refer to the simulation results shown in Fig. 6 when $N_\mathrm{b} = N_\mathrm{b}^{\mathrm{nom}}$.

RESISTIVE-WALL TRANSVERSE COUPLED-BUNCH INSTABILITY

The longitudinal resistive-wall wakefield decays along a distance much shorter than the bucket length in the booster. On the contrary, the transverse resistive-wall wakefield is long-range and can lead to TCBI.

In the following, analytical estimations of the TCBI growth-rate are provided. The needed parameters are taken from Table 1 and a layer thickness of 1µm is assumed as concerns the resistive-wall impedance.

Assuming M_b equally-spaced bunches in the ring, the motion of the entire beam can be considered as the sum of M_b coherent coupled-bunch modes. The transverse growth-rate α_μ for the μ-th coupled-bunch mode, where μ is an integer between 0 and $M_\mathrm{b}-1$, can be easily computed taking into account only the most prominent radial mode in the azimuthal $m = 0$ and assuming Gaussian bunches. The expression for α_μ is [13]

$$\alpha_\mu = -\frac{ceM_\mathrm{b}N_\mathrm{b}f_0}{4\pi E_0 Q_{x,y}} \sum_{q=-\infty}^{\infty} \mathrm{Re}\left[Z_{x,y}\left(f_{\mu,q}\right)\right], \qquad (5)$$

where E_0 is in eV units and $f_{\mu,q} = f_0(qM_\mathrm{b} + \mu + Q_{x,y})$.

Considering the value of $Q_{x,y}^{\mathrm{nom}}$ and the shape of the transverse resistive-wall impedance near plus or minus f_0, it can be seen that the most unstable mode $\bar{\mu}$ satisfies the condition $(qM_\mathrm{b} + \bar{\mu} + Q_{x,y}^{\mathrm{nom}}) \in [-1, 0]$ for a certain q (Fig. 8). This condition is satisfied for $\bar{\mu} = 16370$ and $q = -1$. Note also that for the most unstable and stable modes, equal to

16370 and 16371 respectively, the most significant term in the summation of Eq. (5) comes when $q = -1$.

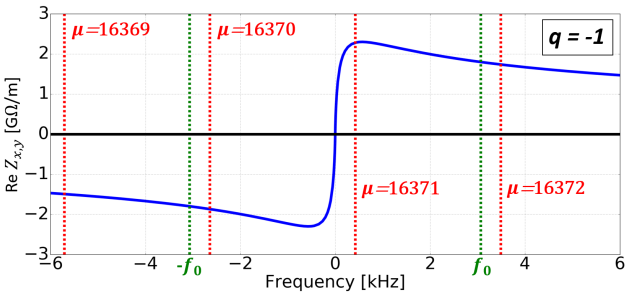

Figure 8: Resistive-wall transverse dipolar impedance (blue) as a function of frequency assuming $\delta_1 = 1\mu m$. The two green lines mark plus or minus f_0. The four red lines mark $f_{\mu,q}$, where $q = -1$, $Q_{x,y} = Q_{x,y}^{\text{nom}}$ and μ varies as shown.

Figure 9 (left) shows α_μ as a function of μ and confirms that $\bar{\mu}$ leads to the largest growth-rate $\alpha_{\bar{\mu}} = 2320$ 1/s.

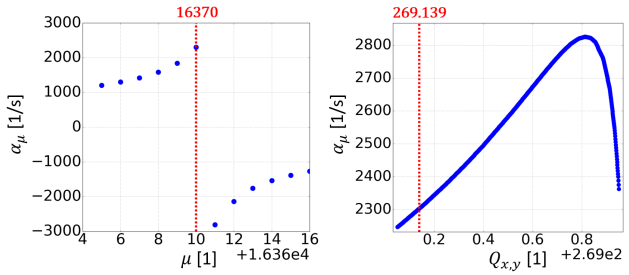

Figure 9: Left: TCBI growth rate, as a function of the coupled-bunch mode, obtained with Eq. (5) assuming $\delta_1 = 1\mu m$. The most unstable mode is marked by a red line. Right: TCBI growth rate as a function of $Q_{x,y}$ with $\lfloor Q_{x,y} \rfloor$=269 and $\mu = 16370$. The value $Q_{x,y}^{\text{nom}}$ is marked by a red line. All the other needed parameters are taken from Table 1.

Figure 9 (right) shows α_μ as a function of $Q_{x,y}$ when $\mu = 16370$ and the integer part of the tune is $\lfloor Q_{x,y} \rfloor$=269. Note that $\mu = 16370$ is the most unstable mode for all these values of $Q_{x,y}$. The plot indicates that the maximum growth rate of 2830 is achieved when $Q_{x,y} = 269.812$.

The value $\alpha_{\bar{\mu}} = 2320$ calculated for the nominal tune corresponds to a TCBI rise-time of 0.435 ms or 1.33 revolution turns. If $Q_{x,y} = 269.812$, then the rise-time is 1.08 turns. These rise-times are shorter than the SR transverse damping-time by several orders of magnitude. Therefore SR cannot help suppressing TCBI.

Transverse bunch-by-bunch feedback systems are usually used in other lepton factories to counteract TCBI [14]. However, these systems cannot act on the short time of one revolution turn. Therefore new feedbacks are required and some schemes have already been proposed [4].

CONCLUSION

The present contribution showed that the first-designed parameters for the FCC-ee booster cannot provide stable beams to the main ring. This is due to the resistive-wall impedance which leads to microwave instability for nominal-intensity beams even if a copper layer is added to the stainless-steel beam pipe for impedance reduction. Therefore, a second mitigation technique was also taken into account, i.e. the increase of the power lost by the beam for synchrotron radiation. This second mitigation is in agreement with the current baseline plans, which foresee the installation of several wigglers in the booster. Using a proper combination of parameters, microwave and transverse-mode-coupling instabilities were not observed for nominal-intensity beams. However, analytical estimations indicated that the transverse-coupled-bunch-instability rise-time is only about one revolution turn making necessary the design of a new feedback system.

ACKNOWLEDGEMENTS

Special thanks go to E. Belli, R. Kersevan, K. Oide and F. Zimmermann for their precious support. This work was partly supported by the European Commission under HORIZON 2020 Integrating Activity project ARIES, Grant agreement nº 730871, and by INFN National committee through the ARYA project.

REFERENCES

[1] A. Abada *et al.*, "FCC-ee: The Lepton Collider," *Eur. Phys. J. ST*, vol. 228, no. 2, pp. 261–623, 2019.

[2] B. Härer, B. Holzer, Y. Papaphilippou, and T. Tydecks, "Status of the FCC-ee Top-Up Booster Synchrotron," no. CERN-ACC-2018-111, p. MOPMF059. 3 p, 2018.

[3] M. Migliorati *et al.*, "Collective Effects in the Booster Synchrotron," FCC Week 2019, Brussels, Belgium, 2019.

[4] A. Drago, "Feedback Systems for FCC-ee," in *Proceedings, 58th ICFA Advanced Beam Dynamics Workshop on High Luminosity Circular e^+e^- Colliders: United Kingdom*, 2017.

[5] "CERN IW2D Code." `https://twiki.cern.ch/twiki/bin/view/ABPComputing/ImpedanceWake2D`.

[6] O. Henry and O. Napoly, "The Resistive Pipe Wake Potentials for Short Bunches," *Part. Accel.*, vol. 35, pp. 235–248, 1991.

[7] E. Shaposhnikova, "Signatures of Microwave Instability," Tech. Rep. CERN-SL-99-008-HRF, Feb 1999.

[8] "CERN BLonD Code." `https://blond.web.cern.ch`.

[9] D. Boussard, "Observation of Microwave Longitudinal Instabilities in the CPS," Tech. Rep. CERN-LabII-RF-INT-75-2, CERN, Geneva, Apr 1975.

[10] R. H. Helm, M. J. Lee, P. L. Morton, and M. Sands, "Evaluation of Synchrotron Radiation Integrals," *IEEE Transactions on Nuclear Science*, vol. 20, pp. 900–901, June 1973.

[11] F. J. Sacherer, "Transverse Bunched Beam Instabilities - Theory," *Conf. Proc.*, vol. C740502, pp. 347–351, 1975.

[12] "CERN DELPHI Code." `https://twiki.cern.ch/twiki/bin/view/ABPComputing/DELPHI`.

[13] K. Y. Ng, *Physics of Intensity Dependent Beam Instabilities*. World Scientific, 2005.

[14] A. Drago *et al.*, "High Current Multibunch Operation at DAΦNE," in *Proceedings of the 2001 Particle Accelerator Conference*, vol. 5, pp. 3543–3545, 2001.